

Effect of Annealing on the Pitting Corrosion Resistance of Anodized Aluminum-Magnesium Alloy Processed by Equal Channel Angular Pressing

In-Joon Son[†], Hiroaki Nakano¹, Satoshi Oue¹, Shigeo Kobayashi²,
Hisaki Fukushima¹, and Zenji Horita¹

*Department of Materials Process Engineering, Graduate School of Engineering, Kyushu University,
744 Motoooka, Nishi-ku, Fukuoka, 819-0395, Japan*

¹*Department of Materials Science & Engineering, Faculty of Engineering, Kyushu University,
744 Motoooka, Nishi-ku, Fukuoka, 819-0395, Japan*

²*Department of Applied Chemistry and Biochemistry, Faculty of Engineering, Kyushu Sangyo University,
2-3-1 Matsukadai, Higashi-ku, Fukuoka, 813-8503, Japan*

The effect of annealing on the pitting corrosion resistance of anodized Al-Mg alloy (AA5052) processed by equal-channel angular pressing (ECAP) was investigated by electrochemical techniques in a solution containing 0.2 mol/L of AlCl₃ and also by surface analysis. The Al-Mg alloy was annealed at a fixed temperature between 473 and 573 K for 120 min in air after ECAP. Anodizing was conducted for 40 min at 100-400 A/m² at 293 K in a solution containing 1.53 mol/L of H₂SO₄ and 0.0185 mol/L of Al₂(SO₄)₃. The internal stress generated in anodic oxide films during anodization was measured with a strain gauge to clarify the effect of ECAP on the pitting corrosion resistance of anodized Al-Mg alloy. The time required to initiate the pitting corrosion of anodized Al-Mg alloy was shorter in samples subjected to ECAP, indicating that ECAP decreased the pitting corrosion resistance. However, the pitting corrosion resistance was greatly improved by annealing after ECAP. The time required to initiate pitting corrosion increased with increasing annealing temperature. The strain gauge attached to Al-Mg alloy revealed that the internal stress present in the anodic oxide films was compressive stress, and that the stress was larger with ECAP than without. The compressive internal stress gradually decreased with increasing annealing temperature. Scanning electron microscopy showed that cracks occurred in the anodic oxide film on Al-Mg alloy during initial corrosion and that the cracks were larger with ECAP than without. The ECAP process of severe plastic deformation produces large internal stresses in the Al-Mg alloy; the stresses remain in the anodic oxide films, increasing the likelihood of cracks. It is assumed that the pitting corrosion is promoted by these cracks as a result of the higher internal stress resulting from ECAP. The improvement in the pitting corrosion resistance of anodized Al-Mg alloy as a result of annealing appears to be attributable to a decrease in the internal stresses in anodic oxide films

Keywords : equal-channel angular pressing, anodizing, pitting corrosion, internal stress, annealing

1. Introduction

Although aluminum is inherently a reactive metal, it shows excellent corrosion resistance over a neutral range of pH 4-8 due to its superficial oxide film. However, in solutions containing Cl⁻, pitting corrosion occurs locally where the oxide film is attacked by Cl⁻.^{1),2)} Therefore, Al alloys are generally anodized with electrolysis to improve such properties as corrosion resistance and hardness.^{3),4)} On the other hand, reducing the grain size of metallic ma-

terials to the submicrometer range or even the nanometer range using the equal-channel angular pressing (ECAP) process is increasingly being studied with the aim of improving mechanical properties such as strength and ductility.⁵⁾⁻⁸⁾ Authors previously reported that the pitting corrosion resistance of anodized Al was improved by ECAP, but the corrosion resistance of anodized Al-Mg alloy was worse with ECAP than without.^{9),10)} The improvement in the pitting corrosion resistance of anodized Al resulting from ECAP appeared to be caused by a decrease in the size of impurity precipitates that act as origins of pitting corrosion. In the case of anodized Al-Mg alloy,

[†] Corresponding author: son@depo.zaiko.kyushu-u.ac.jp

cracks occurred in the anodic oxide films during initial corrosion. The cracks were larger with ECAP than in its absence, suggesting that the pitting corrosion of anodized Al-Mg alloy was promoted by the cracks resulting from ECAP. However, no mechanism has been reported that explains the reduction in pitting corrosion resistance of anodized Al-Mg alloy as a result of ECAP.

In this study, the mechanism of the change in the pitting corrosion resistance of anodized Al-Mg alloy with ECAP was clarified by surface analysis and the internal stress in the anodic oxide film estimated by using a strain gauge. The Al-Mg alloy was subjected to annealing after ECAP in an attempt to improve the pitting corrosion resistance of anodized Al-Mg alloy.

2. Experimental

AA5052 (0.05% Cu, 0.11% Si, 0.24% Fe, 0.01% Mn, 2.5% Mg, 0.01% Zn, 0.17% Cr, <0.15% other elements, rest Al) was used as specimen of Al-Mg alloy. Fig. 1 shows a schematic diagram of the ECAP process. ECAP was conducted for 4 passes at room temperature using a die with a channel angle of 90° , which creates an equivalent strain of ~ 1 during one passage through the die. The sample was rotated by 90° about the longitudinal axis in the same sense between consecutive passes, the generally designated processing route Bc.⁸⁾ The pressings were performed at a rate of $\sim 19 \text{ mms}^{-1}$ using MoS_2 as a lubricant. The initial grain sizes of Al-Mg alloy prior to ECAP were 30 - 50 μm . The average grain sizes of Al-Mg alloy after the ECAP process were confirmed by TEM observation to be 0.2 - 0.5 μm .¹¹⁾

Prior to anodization, Al-Mg alloy was carefully polished down with No.1500 emery paper and immersed in 0.75

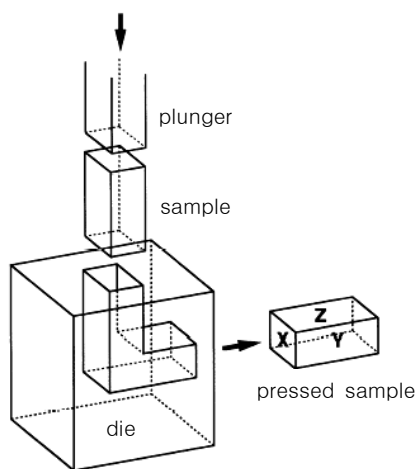


Fig. 1. Schematic diagram of ECAP.

mol/L of NaOH solution at 20°C for 30s, after which it was neutralized in 0.48 mol/L of HNO_3 solution for 30s and electropolished in a 293 K solution containing methanol and perchloric acid ($\text{MeOH} : \text{HClO}_4 = 4 : 1$) at 10 V for 5 min. Anodizing was conducted in a solution containing 1.53 mol/L of H_2SO_4 and 0.0185 mol/L of $\text{Al}_2(\text{SO}_4)_3 \cdot 16\text{H}_2\text{O}$ at 293 K under galvanostatic conditions of 100 - 400 A/m^2 for 40 min, agitated at 100rpm by using a magnetic stirrer. Specimens 10 mm in diameter were prepared for corrosion testing. Their corrosion resistance was investigated over an area 6mm in diameter and the remaining area was sealed with waterproof tape to prevent any corrosion from the edge. After anodized Al-Mg alloy had been immersed in a solution containing 0.2 mol/L of AlCl_3 at 298K for 30 min in an air atmosphere, the time-dependence of anodic current density was measured while being maintained at 1.2V vs. NHE. The electrode potentials were measured using a saturated Ag/AgCl reference electrode (0.199 V vs. NHE, 25°C). In the presentation of anodization and curves of anodic current density, the potentials were plotted with reference to NHE. Platinum was used as the counter-electrode in all electrochemical techniques.

For internal stress measurement, samples of Al-Mg alloy 10 mm in diameter and 0.325 mm in thickness were prepared by using a glow-discharge cutting machine. The specimens were subjected to ultrasonic cleaning in acetone for 10 min and then waterproof-type strain gauges were attached to the rear sides of the specimens with an adhesive and dried for 24 h in air. The internal stress generated in the oxide film during anodization was estimated by measuring the strain in the Al-Mg alloy samples. The tensile and compressive strains in the Al-Mg alloy showed the presence of residual tensile and compressive stress, respectively, in the anodic oxide film. The Al-Mg alloy samples were annealed at a fixed temperature of 473, 523, or 573 K for 120 min in air atmosphere after ECAP. The morphology of anodized Al-Mg alloy with and without ECAP and the morphology of pitting corrosion were analyzed by FE-SEM and SEM.

3. Results and discussion

3.1 Effect of ECAP on the anodization behavior of Al-Mg alloy

Fig. 2 shows the time-dependence of the anode potential of Al-Mg alloy during galvanostatic anodization at various current densities. Fig. 2(b) shows a magnification of the anodizing time on the x-axis of Fig. 2(a). The anode potentials of Al-Mg alloy rapidly shifted to more anodic values at the initial stage, but later moved gradually to the less noble direction and reached an almost constant level. It is known in the formation of porous-type oxide films that the anode potential shifts to the noble direction due to

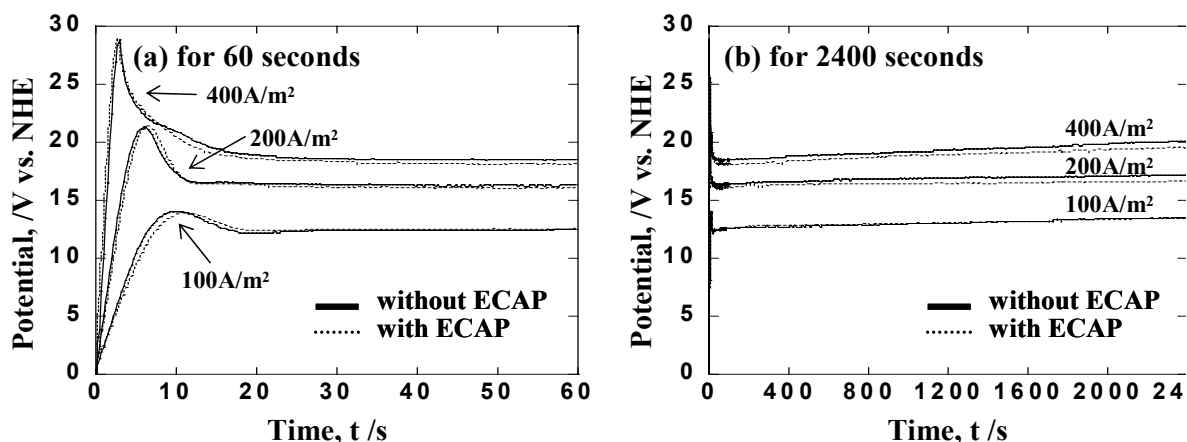


Fig. 2. Time-dependence of anode potential of Al-Mg substrate (a, b) during anodization at various current densities in a solution containing $1.53 \text{ mol}\cdot\text{L}^{-1}$ of H_2SO_4 and $0.0185 \text{ mol}\cdot\text{L}^{-1}$ of $\text{Al}_2(\text{SO}_4)_3$ at 293K.

the formation of barrier-type oxide films during the first stage, then shifts to the less noble direction due to the formation of porous-type oxide films. The time-dependence of the anode potential shown in Fig. 2 indicates the formation of porous-type Al oxide films.⁴⁾ There was very little difference in anode potential of Al-Mg alloy between with ECAP and without. It therefore appears that ECAP has no influence on the formation behavior of oxide films by anodization.

3.2 Morphology of the anodic oxide films

Fig. 3 shows the FE-SEM images of anodized Al-Mg alloy without ECAP and with. Normal area (N) and impurity precipitates (P) were observed in anodized Al-Mg

alloy [(b), (e)]. Although anodic oxide films with porous of about 10 nm in diameter were formed in normal areas [(a), (d)], no oxide films were formed on the impurity precipitates [(c), (f)]. The anodic oxide film were absent at the boundary between the normal oxide films and the impurity precipitates. It was reported previously by the authors that these precipitates in Al-Mg alloy were Si or Fe-Al intermetallic compounds.¹²⁾

3.3 Effect of ECAP and annealing on the pitting corrosion resistance

The time-dependence of the anodic current density of Al-Mg alloy anodized at various current densities is shown in Fig. 4. Samples were held at 1.2 V in the solution con-

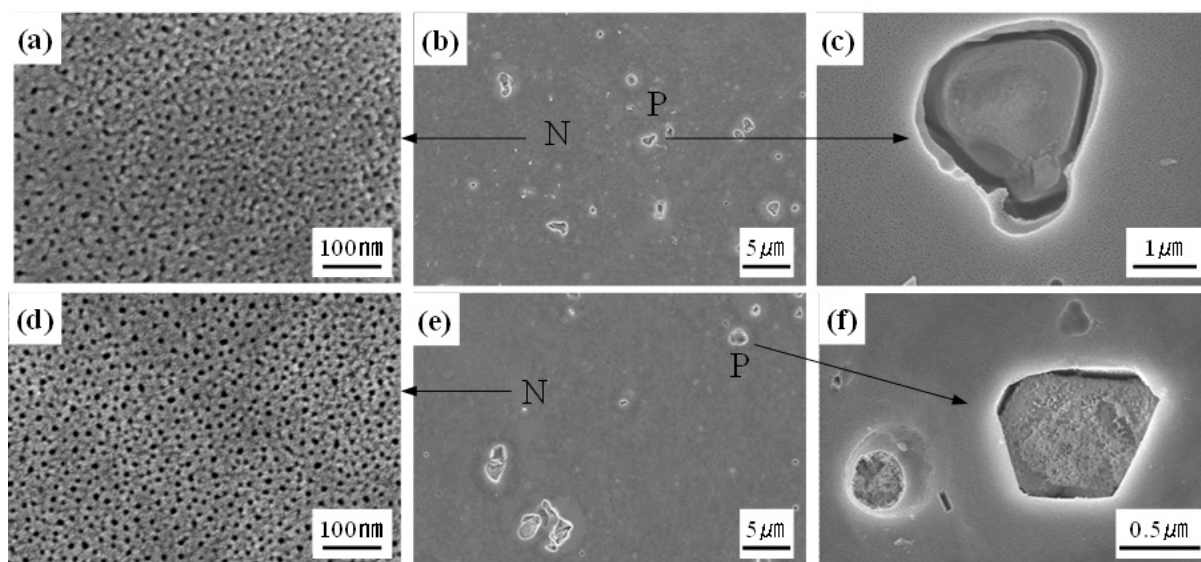


Fig. 3. FE-SEM images of Al-Mg alloy without ECAP (a, b, c) and with (d, e, f) anodized at $400 \text{ A}\cdot\text{m}^{-2}$ for 40 min.

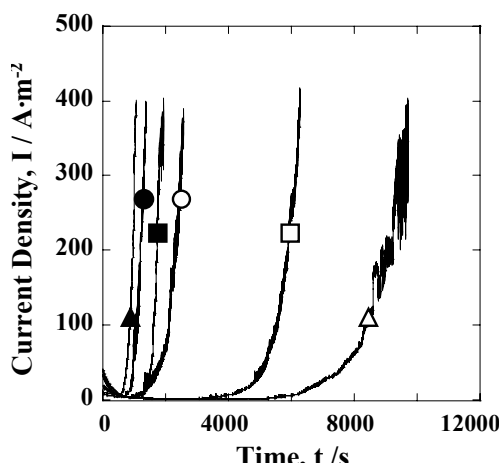


Fig. 4. Time-dependence of the anodic current density of Al-Mg alloy anodized at 100, 200 and 400 A·m⁻² while kept at constant potential of 1.2V in 0.2 mol·L⁻¹ of AlCl₃ solution. ○●: 100 A/m², □■: 200 A/m², △▲: 400 A/m², ○□△: without ECAP, ●●■▲: with ECAP

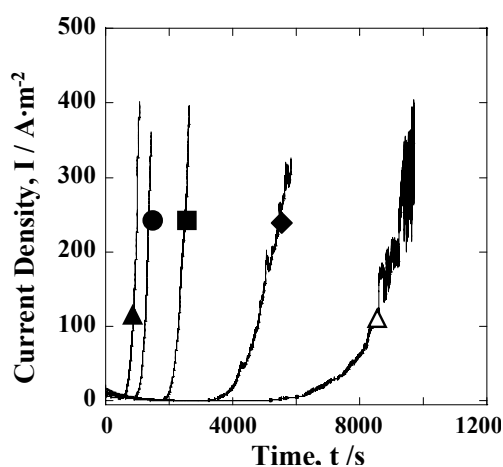


Fig. 5. Effect of annealing on the time-dependence of the anodic current density of Al-Mg alloy anodized at 400 A·m⁻² while kept at constant potential of 1.2V in 0.2 mol·L⁻¹ of AlCl₃ solution. ▲: annealing-free, ●: 473K, ■: 523K, ◆: 573K, △: without ECAP, ▲●■◆: with ECAP

taining 0.2 mol/L of AlCl₃. The anodic current density of anodized Al-Mg alloy increased rapidly after a certain period of time due to the initiation of pitting corrosion. The time required for initiating the pitting corrosion of anodized Al-Mg alloy was longer without ECAP than with, regardless of the anodizing current density, showing that ECAP worsened pitting corrosion resistance. Particularly with increased current density of anodizing, the time to pitting corrosion was greatly shortened by ECAP. The time to pitting corrosion of anodized Al-Mg alloy increased with increased anodizing current density, with the exception of Al-Mg anodized at 400 A/m² with ECAP.

Since anodizing duration was fixed at 40 min in this study, the thickness of anodic oxide films increased with increased anodizing current density. The pitting corrosion resistance was therefore mostly improved with increased anodizing current density.

The Al-Mg alloy samples were annealed at a fixed temperature of 473, 523, or 573 K for 120 min in air after ECAP. Fig. 5 shows the effect of annealing on the time-dependence of the anodic current density of Al-Mg alloy anodized at 400 A·m⁻². The time to pitting corrosion of anodized Al-Mg alloy with ECAP increased with increasing annealing temperature, indicating that the pitting corrosion resistance improved with increasing annealing temperature.

3.4 Morphology of the pitting area

Anodized Al-Mg alloy without ECAP was kept at a constant potential of 1.2 V in 0.2 mol/L of AlCl₃ solution to generate pitting corrosion. The morphology of the pitting area is shown in Fig. 6. It was found from SEM images at an initial stage of pitting corrosion (a,b) that pitting corrosion occurred around the precipitates, and cracks proceeded in anodic oxide films through the pitting area. Since no cracks were present in anodic oxide films before the corrosion test as shown in Figs. 3 (b) and (e), they most likely occur during pitting corrosion. It is clear that the pitting corrosion originates around the precipitates and generates cracks in the anodic oxide films. The initial cracks grew and finally connected with other cracks, forming circles during pitting corrosion. [Figs. 3(c) and 3(d)] Some anodic oxide films with circular cracks were exfoliated, resulting in exposure of the Al-Mg alloy substrate. Anodized Al-Mg alloy with ECAP showed the almost same trend about the surface analysis of pitting areas as anodized Al-Mg alloy without ECAP. The pitting corrosion seems to be accelerated by cracks due to exposure of Al-Mg alloy substrate unprotected by anodic oxide films.

3.5 Effect of ECAP and annealing on the internal stress in anodic oxide films on Al-Mg alloy

Fig. 7 shows the time-dependence of the strain of an Al-Mg alloy sample during anodization at 400 A·m⁻². Although the internal stress generated in the anodic oxide film on the Al-Mg alloy was a tensile stress in the initial stage of anodization, the stress changed to a compressive one after 30 s, irrespective whether the sample had undergone ECAP or not. The compressive stress increased when the electrolytic anodization process was stopped. During the initial 3 min of anodization, there was very little difference in the internal stress of anodic oxide films between

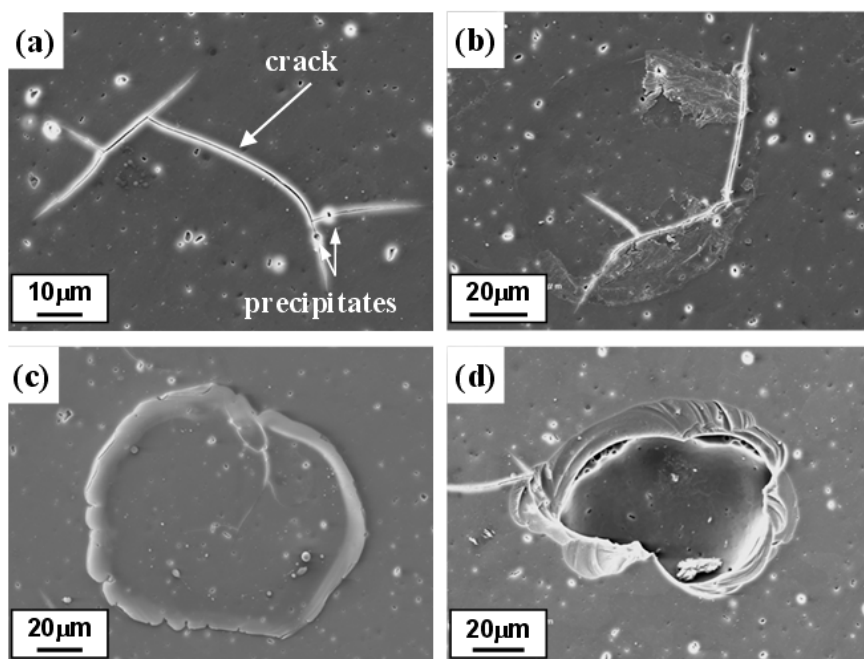


Fig. 6. SEM images of anodized Al-Mg alloy without ECAP after kept 1.2V in 0.2 mol·L⁻¹ of AlCl₃ solution.

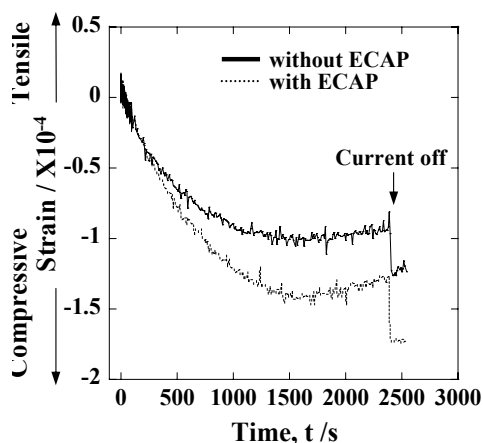


Fig. 7. Time-dependence of strain of Al-Mg alloy substrates during anodization at 400 A·m⁻² in a solution containing 1.53 mol·L⁻¹ of H₂SO₄ and 0.0185 mol·L⁻¹ of Al₂(SO₄)₃ at 293K.

samples subjected to ECAP and those not subjected to ECAP. After 3 min, however, the internal stress was higher with ECAP than without, showing that ECAP increased the residual stress in anodic oxide films on Al-Mg alloy.

Al-Mg alloy was annealed at various temperatures after ECAP and the internal stress in the anodic oxide films was investigated during anodization. Fig. 8 shows the effect of the annealing temperature on the strain in Al-Mg alloy. The internal stress of anodic oxide films was a compressive one for all annealing temperatures and decreased with increasing annealing temperature: annealing, there

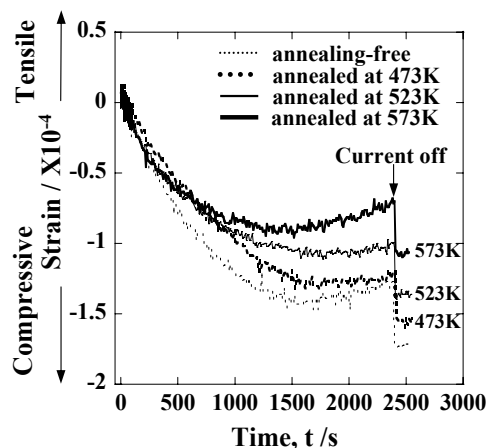


Fig. 8. Effect of annealing on the strain of Al-Mg substrates during anodization at 400 A·m⁻² in a solution containing 1.53 mol·L⁻¹ of H₂SO₄ and 0.0185 mol·L⁻¹ of Al₂(SO₄)₃ at 293K.

fore, decreased the residual internal stress in anodic oxide films.

3.6 Factors affecting the internal stress of anodic oxide films

Fig. 9 shows the X-ray diffraction patterns of samples of Al-Mg alloy subjected to ECAP and annealed at various temperatures. Although the X-ray diffraction of the (311) was shifted to the large 2 θ direction by ECAP, it shifted back to the small 2 θ direction on increasing the annealing temperature. Table 1 shows the lattice constants of Al-Mg

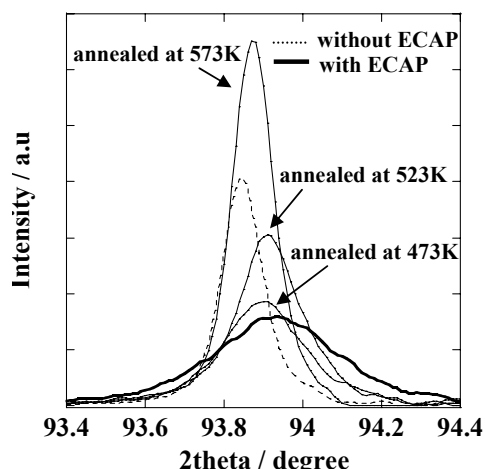


Fig. 9. Effect of annealing on the X-ray diffraction pattern of Al-Mg alloy processed by ECAP.

Table 1. Lattice constants of Al-Mg alloy calculated by X-ray diffraction.

Al-Mg alloy	2 θ [degree]	Intensity [cps]	$d_{(311)}$ [Å]	half width [deg]	Lattice constant by $d_{(311)}$ [Å]
Without ECAP	93.85	2022	1.2246	0.129	4.0613
With ECAP	93.94	795	1.2237	0.360	4.0584
ECAP+473K annealing	93.91	852	1.2240	0.231	4.0594
ECAP+523K annealing	93.91	1519	1.2240	0.198	4.0594
ECAP+573K annealing	93.89	3254	1.2242	0.128	4.0601

alloy, calculated from X-ray diffraction patterns. Although the lattice constant of Al-Mg alloy calculated from the 2θ value of the (311) decreased as a result of ECAP, it increased with increasing annealing temperature. The X-ray diffraction patterns of Al-Mg alloy showed that compressive internal stress is generated in Al-Mg alloy by ECAP, and relieved by the application of annealing.

When the anodic oxide films are formed on metal, an internal stress is generally produced in oxide films due to difference in molar volume between metal substrate and oxide film. It has been reported that a compressive internal stress remains in oxide films of the $\text{Al}_2\text{O}_3/\text{Al}$ system, the Pilling-Bedworth ratio (the ratio of the molar volume of the oxide film to that of the metal substrate) is 1.28 (exceeding 1.0).¹³⁾ Because the anodic oxide films on Al cannot expand as a result of the constraint of the substrate, the compressive stress in anodic oxide films remains, despite them having a Pilling-Bedworth ratio of more 1.0: this effect was also found in this study.

Pitting corrosion occurred around the precipitates, irrespective of the ECAP or not and cracks proceeded in anodic oxide films through the pitting area. It is assumed that

anodic oxide films are free from constraint by the substrate in the pitting corrosion area around precipitates and, consequently, tensile stress is generated locally in oxide films, resulting in propagation of cracks. The ECAP process of severe plastic deformation applies a compressive internal stress to the Al-Mg alloy, as seen from X-ray diffraction patterns in Fig. 9. The Pilling-Bedworth ratio is increased by ECAP, because ECAP decreases the lattice constant of the Al-Mg alloy. Therefore, the compressive stress generated in anodic oxide films on Al-Mg alloy was larger with ECAP than without. With increasing the compressive stress in anodic oxide films, cracks occurred more readily in oxide films during initial pitting corrosion. The pitting corrosion seems to be accelerated by cracks due to exposure of Al-Mg alloy substrate unprotected by anodic oxide films.

The pitting corrosion resistance of anodized Al-Mg alloy was greatly decreased by the application of ECAP. It appears that the higher compressive internal stress of Al-Mg alloy resulting from ECAP is also likely to remain in anodic oxide films, increasing the likelihood of cracks. The resistance to pitting corrosion of anodized Al-Mg alloy with ECAP gradually improved with increased annealing temperature. The improvement caused by annealing appears to be attributable to decreased cracking in anodic oxide films as a result of the lower internal stress in the annealed Al-Mg alloy.

4. Conclusions

The effect of annealing on the pitting corrosion resistance of anodized Al-Mg alloy processed by ECAP was investigated by electrochemical techniques and by surface analysis. The time required to initiate the pitting corrosion of anodized Al-Mg alloy was shorter in samples subjected to ECAP, indicating that ECAP decreased the pitting corrosion resistance. However, the pitting corrosion resistance was greatly improved by annealing after ECAP. The time required to initiate pitting corrosion increased with increasing annealing temperature. The strain gauge attached to Al-Mg alloy revealed that the internal stress present in the anodic oxide films was compressive stress, and that the stress was larger with ECAP than without. The compressive internal stress gradually decreased with increasing annealing temperature. Scanning electron microscopy showed that cracks occurred in the anodic oxide film on Al-Mg alloy during initial corrosion and that the cracks were larger with ECAP than without. The ECAP process of severe plastic deformation produces large internal stresses in the Al-Mg alloy; the stresses remain in the anodic oxide films, increasing the likelihood of cracks. It is

assumed that the pitting corrosion is promoted by these cracks as a result of the higher internal stress resulting from ECAP. The improvement in the pitting corrosion resistance of anodized Al-Mg alloy as a result of annealing appears to be attributable to a decrease in the internal stresses in anodic oxide films.

References

1. H.H. Uhlig, Corrosion and Corrosion Control (in Japanese, p.320, Sangyo Tosho, Tokyo, 1968.
2. G. Ito, Corrosion Science and Engineering (in Japanese), p.306, Corona Publishing Co., Tokyo, 1973.
3. T. Asada, *J. Met. Finish. Soc., Jpn*, **21**, 490 (1970).
4. N. Baba, Anodic Oxide Films Produced by Electrolysis (in Japanese), p.14, Maki Syoten, Tokyo, 1996.
5. R.Z. Valiev, N.A. Krasilnikov and N.K. Tsenev, *Mater. Sci. Eng.*, **A137**, 35-41 (1991).
6. R.Z. Valiev, R.K. Islamgaliev and I.V. Alexandrov, *Prog. Mater. Sci.*, **45**, 103 (2000).
7. Y.T. Zhu, T.G. Langdon, R.S. Mishra, S.L. Semiatin, M.J. Saran and T.C. Lowe, Ultrafine Grained Materials II, The Minerals, Metals & Materials Society, Warrendale (2002)
8. Z. Horita, M. Furukawa, M. Nemoto and T.G. Langdon, *Mater. Sci. Tech.*, **16**, 1239 (2000).
9. I.J. Son, H. Nakano, S. Oue, S. Kobayashi, H. Fukushima and Z. Horita, *J. Japan Inst. Metal.*, **70**, 534 (2006).
10. I.J. Son, H. Nakano, S. Oue, S. Kobayashi, H. Fukushima and Z. Horita, *Mater. Trans.*, **48**, 21 (2007).
11. Z. Horita, T. Fujinami, M. Nemoto and T.G. Langdon, *Metallurgical and Mater. Trans.*, **A 31A**, 691 (2000).
12. I.J. Son, H. Nakano, S. Oue, S. Kobayashi, H. Fukushima and Z. Horita, *Mater. Trans.*, **47**, 1163 (2006).
13. M. Seo and K. Ueno, *J. Finish. Soc. Jpn.*, **51**, 365 (2000).